21

Nano Structural Properties of Lead Doped Cadmium Sulfide (Cd1-xPbxS) Thin Films Deposited by Spray Pyrolysis Technique

Ranojit Kumar Dutta [1,2,3,*]

[1] Faculty of Science and Engineering, City University, Dhaka 1216, Bangladesh.

[2] Department of Physics, Faculty of Engineering, Bangladesh University of Engineering and Technology (BUET), Dhaka 1000, Bangladesh

[3] College of Hydraulic & Environmental Engineering, China Three Gorges University, Yichang, 443002, Hubei, P.R. China.

Abstract: Lead doped cadmium sulfide thin films $Cd_{1-x}Pb_xS$ ($0 \leq x \geq 0.20$) were deposited onto a glass substrate at a temperature of 523K at a low cost spray pyrolysis technique. They were characterized by their structural and optical properties energy dispersive x-ray analysis, scanning electron microscopy and x-ray diffraction. X-ray diffraction patterns of the films are identified as (100), (002), (101), (102), (110), (103) and (201) planes which have hexagonal crystal structure. No extra peak developing occurs with the increasing Pd concentration. The direct band gap energy of the film depends on the concentration. This value varies from 2.52 eV to 2.17 eV as required for solar cell and opto-electronic device applications.

Keywords: Nano Structural Properties, Optical Properties, Spray Pyrolysis, CdS and PbS, Semiconductors.

1 Introduction

CdS and PbS are sensitive to light. Based on their practical application, a study of their mixed thin film structure as spray pyrolysis converters is of technically important (Kamruzzaman et al., 2012). For the preparation CdS and Pb doped CdS thin films, a variety of deposition techniques, including Chemical Bath Deposition technique (CBD) (Guire et al., 2013; Hop et al., 2019; Li, 2015; Salamon, 2016; Saravanakumar et al., 2017), aqueous synthesis (Arshad et al., 2016; Gaponik and Rogach, 2008), precipitation technique (Dalas et al., 1991; Singh & Chauhan, 2009) and quenching method (Butwong et al., 2011) have been used. Spray pyrolysis deposition technique has been a viable technique to produce Cd1-xPbxS films because it several advantages such as low cost experimental set up, high spatial selectivity, precise control over maneuvering the impurity concentration and possibility to overcome the solubility limit (Kamruzzaman et al., 2012; Mahmood et al., 2018; Margoni et al., 2018; Mata et al., 2018; Moumen et al., 2018; Polivtseva et al., 2014).

The present paper aims to investigate the optical band gap prepared by lead doped cadmium sulfide thin films deposited onto a glass substrate at a temperature of 523K using a cos-effective spray pyrolysis technique.

2 Material and Methods

2.1 Experimental Details

Lead doped cadmium sulfide thin films $Cd_{1-x}Pb_xS$ ($0 \leq x \geq 0.20$) were prepared using a low cost spray pyrolysis technique. Aqueous solutions of 0.1M cadmium acetate, Cd $(CH_3COO)_2.3H_2O$, 0.2M thiourea (NH_2CSNH_2) and 0.1M lead acetate, $Pb(CH_3 COO)_2 .2H_2O$ were taken as sources of Cd, S and Pb respectively. A considerable amount of (100

ml) solution was taken in the Beaker. The clean substrate (5cm×2cm) with a suitable mask was put on the susceptor of the heater. The distance between the tip of the nozzle and the surface of the glass substrate was kept at 25 cm. The substrate temperature was measured through placing a copper constantan thermocouple. Thin film condensation involves three distinguished mechanisms depending on the strength of interaction among the atoms of the growing film and that among the atoms of the film and substrate.

3 Results and Discussion

3.1 Structural Properties

X-ray diffraction patterns of the films are shown in Fig. 1. Some peaks, identified as (100), (002), (101), (102), (110), (103) and (201) planes, matched the standard (JCPDS data card 41-1049, a=4.140Å and c=4.140Å) of CdS hexagonal crystal structure. No extra peak developing occurs when Pd concentration increases. The lattice parameters were estimated for (100) and (002) planes using the following relation (1)

$$\frac{1}{d_{hkl}} = \left[\frac{4}{3} \frac{(h^2 + hk + k^2)}{a^2} + \frac{l^2}{c^2} \right]^{\frac{1}{2}} \tag{1}$$

The estimated lattice parameters 'a' and 'c', c/a and volume are presented in Table 1. X-ray diffraction patterns of the $Cd_{1-x}Pb_xS$ thin film are shown in Fig. 1.The table reveals that the average c/a ratio is close to 1.626. The value of 'a' increases, but the value of 'c' decreases. These results imply that the Pb^{2+} has been substituted into the crystal lattice of CdS. As the ionic radius of Pb^{2+} (1.18 Å) is larger than that of Cd^{2+} (0.97 Å), the Pb^{2+} ions have been substituted into the crystal lattice of CdS and caused distortion in CdS lattice. The estimated lattice parameters are very close to the standard value. The synthesised films have wurtzite hexagonal structure. The grain size of the prepared film was estimated for the strongest peak (002) using Scherrer formula (2)

$$D_g = \frac{0.9\lambda}{\Delta \cos \theta} \tag{2}$$

Dg is the average grain size, λ denotes the wavelength of the radiation used as the primary beam of Kα (λ= 1.54178 Å), θ is the angle of incidence in degree and Δ denotes the full width at half maximum (FWHM) of the peak in radian, which was experimentally defined after the correction of instrumental broadening (it is 0.05º in the present case). The average grain size of films is between 4 nm and 9 nm indicating the nanometric size of CdS grains developed in the film.
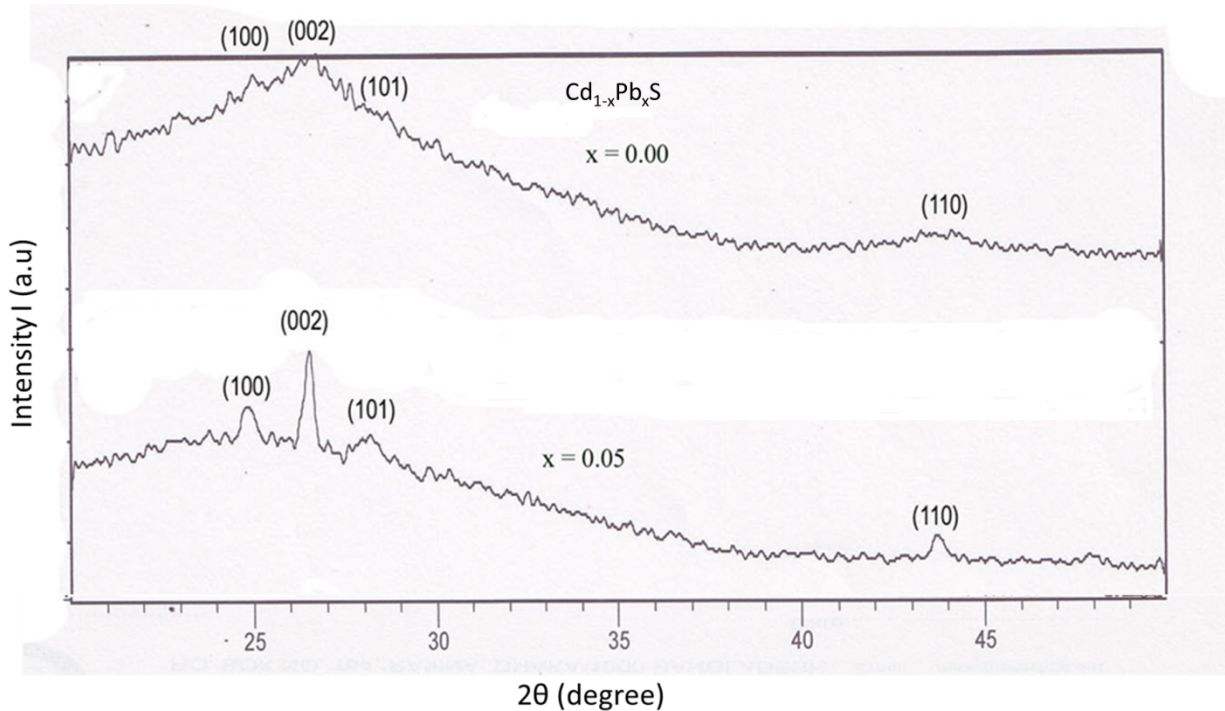

Fig. 1: X-ray diffraction patterns of the $Cd_{1-x}Pb_xS$ thin films.

Table 1: Lattice constants, *c/a* ratio and volume of $Cd_{1-x}Pb_xS$ thin films.

Doping concentrations, X	Lattice constants		c/a ratio	Volume of CdS ($Å^3$)
	A (Å)	C (Å)		
X=0.00	4.125	6.720	1.629	99.022
X=0.05	4.127	6.718	1.627	99.089

Energy dispersive x-ray analysis (EDX) of the films is shown in Fig. 2. There is an atomic percentage of Cd and S for x=0.00 that confirms the CdS, film but there are values of Cd, S and Pb for x = 0.05.The deposited films are $Cd_{1-x}Pb_xS$. The atomic percentage of Cd decreases when increasing Pb concentrations increase (Fig. 3), indicating the incorporation of Pb into the system. The Fig. 3 shows that Cd, S and Pb are present but the films are non-stoichiometric in composition. EDX analysis shows that the films are cadmium rich Fig. 3. This may occur because the reactivity of cadmium is greater than sulpher and lead ions. Scanning Electron Microscope (SEM) micrographs under 10000 magnification of the films are shown in Fig. 2 (a) and Fig. 2 (b). The films are polycrystalline in nature and deposition covers the substrate well. It also exhibits that the cluster formation in the films increases with Pb doping concentration and temperature. For pure CdS, there is no precipitation of Pb, but for x=0.05, precipitation of Pb is observed in Fig. 3 (a) and Fig. 3 (b).
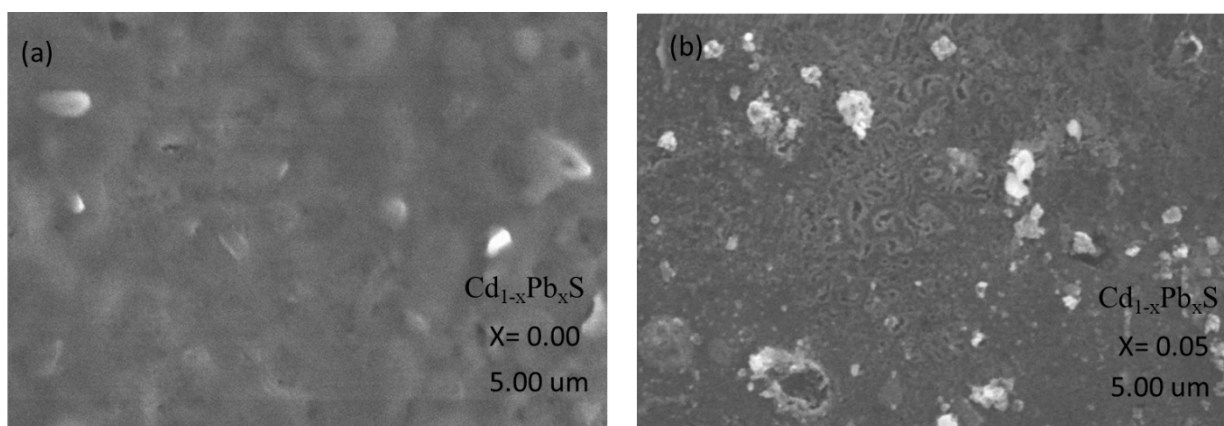
Fig. 2: SEM micrograph of $Cd_{1-x}Pb_xS$, where x = 0.00 as deposited film (0.1M) at 300^0C for 10 min.
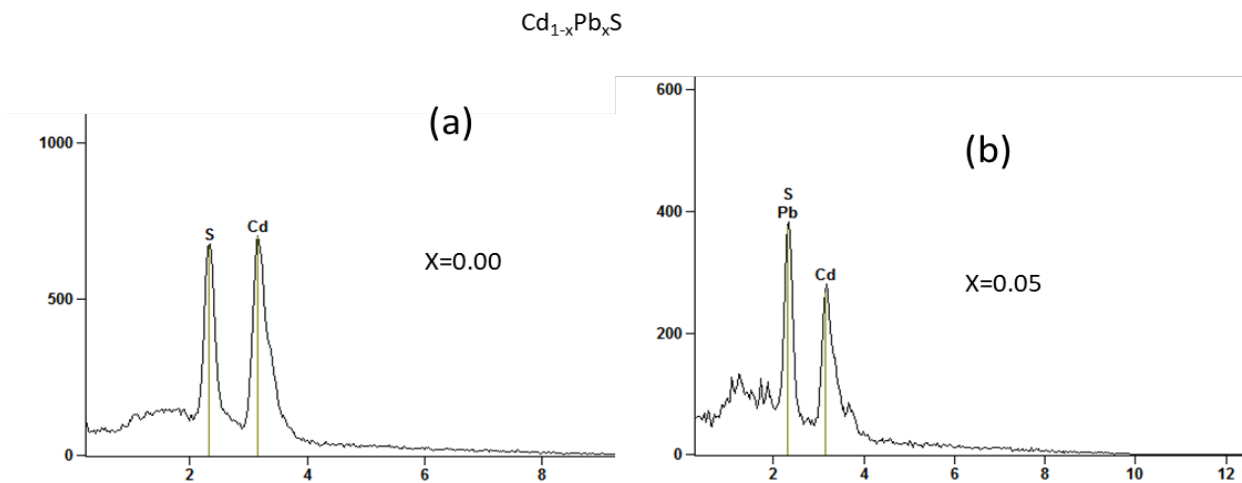
Fig. 3: EDX spectrum of a $Cd_{1-x}Pb_xS$, x=0.00, thin films.

3.2 Optical Properties

The optical properties of the films were investigated within the wavelength range 380 nm to 1100 nm which has illustrated the interaction between photon energies and films structure or among energy configurations. The optical absorption spectra of these films were taken to evaluate the absorption coefficient (α), band gap energy (E_g) and nature of transition involved. Fig. 4 shows the wavelength dependence on the absorption coefficient of the films. Fig. 4 reveals that the optical absorption coefficient, (α) is greater than 105 cm^{-1} for all the films. Also this value increases with Pb doping concentration. This may occur because the films involve several defects. The theory of optical absorption demonstrate the relationship between the absorption coefficient (α) and the photon energy (hυ) as follows:

$$\alpha h\upsilon = A\,(h\upsilon - E_g)^{\wedge}n \qquad (3)$$

α denotes the absorption coefficient, hv denotes the photon energy, E_g denotes the optical band gap and A is the constant which is related to the effective masses associated with the valance band and the conduction band. The factor n assumes values of 1/2, 2, 3/2 and 3 for allowed direct, allowed indirect, forbidden direct, and forbidden indirect transitions, respectively. For the allowed direct type of transitions

$$\alpha h\upsilon = A\,(h\upsilon - E_g)^{\wedge}(1/2) \qquad (4)$$

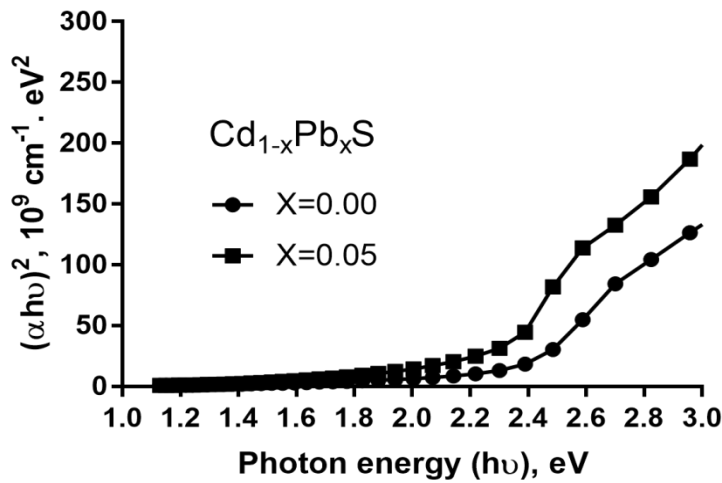The modes of optical transition in these films have been analyzed as shown in Fig. 5.

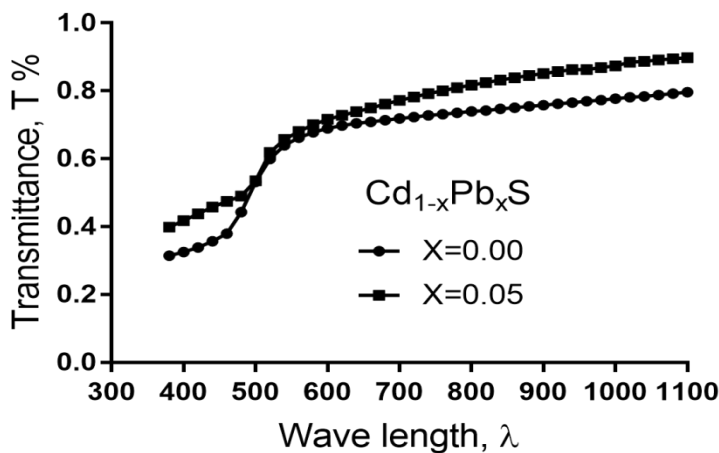**Fig. 4:** Variation of band gap with photon energy for Cd$_{1-x}$Pb$_x$S thin films.

Fig. 5: Variation of optical transmittance with wavelength of Cd$_{1-x}$Pb$_x$S films.

The optical band gap of pure CdS is 2.39 eV and decreases to 2.20 eV as the composition parameter 'x' increases from 0 to 0.05 indicating that a small amount of Pb incorporation affects the optical band gap. This variation of the band gap energy benefit in designing a suitable window material in fabrication for solar cells.

4 Conclusion

The films are polycrystalline in nature with wurtzite hexagonal structure and the grain sizes varied from 4 nm to 9 nm. X-ray diffraction patterns of the films are identified as (100), (002), (101), (102), (110), (103) and (201) planes. No extra peak developing occurs with the increasing Pd concentration. The optical studies showed that the absorption coefficient (α), is very high (105 cm^{-1}). The direct band gap energy of the films is dependent on the concentration (x). This value varies from 2.52 eV to 2.17 eV as required for solar cell and opto-electronic device applications.

References

[1] Arshad, A., Akram, R., Iqbal, S., Batool, F., Iqbal, B., Khalid, B., Khan, A.U., 2016. Aqueous synthesis of tunable fluorescent, semiconductor CuInS2 quantum dots for bioimaging. Arabian Journal of Chemistry.

[2] Butwong, N., Noipa, T., Burakham, R., Srijaranai, S., Ngeontae, W., 2011. Determination of arsenic based on quenching of CdS quantum dots fluorescence using the gas-diffusion flow injection method. Talanta., **85**, 1063-1069, 2011.

[3] Dalas, E., Kallitsis, J., Sakkopoulos, S., Vitoratos, E., Koutsoukos, P.G., 1991. Cadmium sulfide precipitation in aqueous media: Spontaneous precipitation and controlled overgrowth on polyaniline. Journal of Colloid and Interface Science., **141**, 137-145, 1991.

[4] Gaponik, N., Rogach, A.L., 2008. Aqueous synthesis of semiconductor nanocrystals, in: Rogach, A.L. (ed.), Semiconductor Nanocrystal Quantum Dots: Synthesis, Assembly, Spectroscopy and Applications. Springer Vienna, Vienna., 73-99, 2008.

[5] Guire, M.R.D., Bauermann, L.P., Parikh, H., Bill, J., 2013. Chemical Bath Deposition, in: Schneller, T., Waser, R., Kosec, M., Payne, D. (eds.), Chemical Solution Deposition of Functional Oxide Thin Films. Springer Vienna, Vienna, 319-339, 2013.

[6] Hop, X., Van Trinh, H., Quang Dat, K., Quoc Bao, P., 2019. Growth of CdS thin films by chemical bath deposition technique., 2019.

[7] Kamruzzaman, M., Dutta, R., Podder, J., 2012. Synthesis and characterization of the as-deposited Cd1 − xPbxS thin films prepared by spray pyrolysis technique. Semiconductors., **46**, 957-961, 2012.

[8] Li, J., 2015. Preparation and properties of CdS thin films deposited by chemical bath deposition. Ceramics International., **41**, S376-S380, 2015.

[9] Mahmood, W., Ali, J., Zahid, I., Thomas, A., ul Haq, A., 2018. Optical and electrical studies of CdS thin films with thickness variation. Optik., **158**, 1558-1566, 2018.

[10] Margoni, M.M., Mathuri, S., Ramamurthi, K., Ramesh Babu, R., Sethuraman, K., 2018. Modification on the properties of vanadium oxide films deposited from NH4F added HNO3 treated ammonium metavanadate precursor solution by spray pyrolysis technique. Thin Solid Films., **655**, 62-69, 2018.

[11] Mata, V., Maldonado, A., de la Luz Olvera, M., 2018. Deposition of ZnO thin films by ultrasonic spray pyrolysis technique. Effect of the milling speed and time and its application in photocatalysis. Materials Science in Semiconductor Processing., **75**, 288-295, 2018.

[12] Moumen, A., Hartiti, B., Comini, E., El khalidi, Z., Arachchige, H.M.M.M., Fadili, S., Thevenin, P., 2018. Preparation and characterization of nanostructured CuO thin films using spray pyrolysis technique. Superlattices and Microstructures.

[13] Polivtseva, S., Acik, I.O., Katerski, A., Mere, A., Mikli, V., Krunks, M., 2014. Spray Pyrolysis Deposition of SnxSy Thin Films. Energy Procedia., **60**, 156-165, 2014.

[14] Salamon, F., 2016. Effect some Factors on the Structural Properties of the CdS Thin Films Prepared by Chemical Bath Deposition. International Letters of Chemistry, Physics and Astronomy., **64**, 1-10, 2016.

[15] Saravanakumar, S., Chandramohan, R., Premarani, R., Devadasan, J.J., Thirumalai, J., 2017. Studies on Dilute Magnetic Semiconducting Co-Doped CdS Thin Films Prepared by Chemical Bath Deposition method. Journal of Materials Science: Materials in Electronics **28**, 12092-12099, 2017.

[16] Singh, V., Chauhan, P., 2009. Structural and optical characterization of CdS nanoparticles prepared by chemical precipitation method. Journal of Physics and Chemistry of Solids., **70**, 1074-1079, 2009.